# Upper critical field in noncentrosymmetric superconductors

K. V. Samokhin
*Department of Physics, Brock University, St. Catharines, Ontario, Canada L2S 3A1*
(Received 22 May 2008; revised manuscript received 31 October 2008; published 23 December 2008)

We calculate the upper critical field in superconductors without inversion symmetry at arbitrary temperatures in the presence of scalar impurities. Both orbital and spin (paramagnetic) mechanisms of pair breaking are considered. The superconducting phase transition at nonzero field occurs into a helical vortex state, in which the order parameter is modulated along the applied field (in a cubic crystal). The helical state is stable with respect to disorder. However, if the difference between the densities of states in the electron bands that are split by spin-orbit coupling is neglected, then the order-parameter modulation is present only at low temperatures, and only if the system is sufficiently clean and paramagnetically limited. This state resembles the Larkin-Ovchinnikov-Fulde-Ferrell state in centrosymmetric superconductors.

DOI: 10.1103/PhysRevB.78.224520 PACS number(s): 74.20.−z, 74.25.Op, 74.25.Dw

## I. INTRODUCTION

Recently, superconductivity has been discovered in a number of noncentrosymmetric compounds. Physical properties of these materials vary considerably from $CePt_3Si$ (Ref. 1), in which strong electron correlations are responsible for a heavy-fermion behavior and the superconductivity is likely anisotropic with gap nodes, to $Li_2Pd_3B$ and $Li_2Pt_3B$ (Ref. 2), which show rather conventional features, described by the Bardeen-Cooper-Schrieffer (BCS) theory of phonon-mediated pairing.

The absence of inversion symmetry in the crystal lattice brings about important qualitative changes, both in normal and superconducting properties, compared with the centrosymmetric case. These differences are highlighted, in particular, by different responses to an external magnetic field. Distinctive features of noncentrosymmetric superconductors include a strongly anisotropic spin susceptibility with a large residual component,[3–9] magnetoelectric effect,[3,10–12] and nonuniform ("helical") superconducting states.[13–15]

In this paper, we extend the classic theory of the upper critical field, $H_{c2}(T)$, in BCS superconductors, which was developed in Refs. 16 and 17 (see also Ref. 18), to the noncentrosymmetric case. The spin-orbit (SO) coupling of electrons with a noncentrosymmetric crystal lattice considerably changes the nature of single-electron states, lifting spin degeneracy of the energy bands. This modifies the Zeeman coupling of band electrons with magnetic field, which in turn affects the paramagnetic pair breaking. The magnetic phase diagram of noncentrosymmetric superconductors has been previously studied in a two-dimensional case,[19,20] in which the orbital effects are not important. In Ref. 15, the upper critical field for a three-dimensional Rashba superconductor was calculated in the absence of impurities. The effects of disorder on $H_{c2}$ in the Ginzburg-Landau regime near the zero-field critical temperature have been investigated in Ref. 21 for an arbitrary pairing symmetry but without paramagnetic effects. In this paper, we include both orbital and paramagnetic mechanisms of pair breaking, as well as scalar disorder, at arbitrary temperatures. We consider a "minimal" model of a three-dimensional weak-coupling superconductor of cubic symmetry with an isotropic parabolic band split in two by the SO coupling. We assume that the ratio of the SO band splitting to the Fermi energy is small (which is the case in most known noncentrosymmetric materials), and neglect the impurity-induced mixing of the singlet and triplet components of the gap function.

The paper is organized as follows: In Sec. II, we derive the equations for $H_{c2}(T)$, relegating some of the technical details to the Appendix. In Sec. III, the transition temperature as a function of the external field is calculated in the Ginzburg-Landau region near the zero-field critical temperature $T_{c0}$. In Sec. IV, we consider the purely paramagnetic limit, both in the clean and disordered cases. The general case, with the orbital pair breaking included, is studied in Sec. V. Section VI contains a discussion of our results. Throughout the paper we use the units in which $\hbar=k_B=1$.

## II. BASIC EQUATIONS

Let us consider a noncentrosymmetric superconductor with the Hamiltonian given by $H=H_0+H_{\rm imp}+H_{\rm int}$. The first term,

$$H_0=\sum_{\boldsymbol{k}}[\epsilon_0(\boldsymbol{k})\delta_{\alpha\beta}+\boldsymbol{\gamma}(\boldsymbol{k})\boldsymbol{\sigma}_{\alpha\beta}]a^\dagger_{\boldsymbol{k}\alpha}a_{\boldsymbol{k}\beta}, \tag{1}$$

describes noninteracting electrons in the crystal lattice potential, where $\alpha,\beta=\uparrow,\downarrow$ are spin indices, $\epsilon_0(\boldsymbol{k})$ is the quasiparticle energy, and $\hat{\boldsymbol{\sigma}}$ are the Pauli matrices. We assume a parabolic band and include the chemical potential in the dispersion function: $\epsilon_0(\boldsymbol{k})=\boldsymbol{k}^2/2m^*-\epsilon_F$, where $m^*$ is the effective mass, $\epsilon_F=k_0^2/2m^*$, and $k_0$ is the Fermi wave vector in the absence of the SO coupling. In Eq. (1) and everywhere below, summation over repeated spin indices is implied while summation over band indices is always shown explicitly.

The second term in Eq. (1) describes a Rashba-type SO coupling of electrons with the crystal lattice.[22] We focus on the case of a noncentrosymmetric cubic crystal with the point-group $\mathbb{G}=\mathbf{O}$, which is applicable, for instance, to $Li_2(Pd_{1-x},Pt_x)_3B$. The simplest expression for the SO coupling compatible with all symmetry requirements has the following form:

 

$$\boldsymbol{\gamma}(\boldsymbol{k}) = \gamma_0 \boldsymbol{k}, \tag{2}$$

where $\gamma_0$ is a constant. It is convenient to characterize the SO coupling strength by a dimensionless parameter,

$$\varrho = \frac{m^*|\gamma_0|}{k_0}. \tag{3}$$

Diagonalization of the Hamiltonian (1) yields two nondegenerate bands labeled by helicity $\lambda = \pm$, which are described by the following dispersion functions:

$$\xi_\lambda(\boldsymbol{k}) = \epsilon_0(\boldsymbol{k}) + \lambda|\boldsymbol{\gamma}(\boldsymbol{k})| = \frac{k^2 - k_0^2}{2m^*} + \lambda|\gamma_0|k. \tag{4}$$

The SO band splitting is given by $E_{\mathrm{SO}} = 2|\gamma_0|k_0$, therefore $\varrho = E_{\mathrm{SO}}/4\epsilon_F$. While the two Fermi surfaces, defined by the equations $\xi_\lambda(\boldsymbol{k}) = 0$, have different radii: $k_{F,\lambda} = k_0(\sqrt{1+\varrho^2} - \lambda\varrho)$, the Fermi velocities are the same: $\boldsymbol{v}_\lambda = v_F\hat{\boldsymbol{k}}$, where $v_F = (k_0/m^*)\sqrt{1+\varrho^2}$.

Scattering of electrons at isotropic scalar impurities is introduced according to

$$H_{\mathrm{imp}} = \int d^3\boldsymbol{r} U(\boldsymbol{r}) \psi_\alpha^\dagger(\boldsymbol{r}) \psi_\alpha(\boldsymbol{r}), \tag{5}$$

where the impurity potential $U(\boldsymbol{r})$ is a random function with zero mean and the correlator $\langle U(\boldsymbol{r}_1)U(\boldsymbol{r}_2)\rangle = n_{\mathrm{imp}}U_0^2\delta(\boldsymbol{r}_1 - \boldsymbol{r}_2)$, $n_{\mathrm{imp}}$ is the impurity concentration, and $U_0$ has the meaning of the strength of an individual pointlike impurity. The field operators have the usual form: $\psi_\alpha(\boldsymbol{r}) = \mathcal{V}^{-1/2}\Sigma_{\boldsymbol{k}} e^{i\boldsymbol{k}\boldsymbol{r}} a_{\boldsymbol{k}\alpha}$, where $\mathcal{V}$ is the system volume.

We assume that there is a local attraction between electrons, e.g., due to phonons, and describe the Cooper pairing by a BCS-like Hamiltonian:

$$H_{\mathrm{int}} = -V \int d^3\boldsymbol{r} \psi_\uparrow^\dagger(\boldsymbol{r}) \psi_\downarrow^\dagger(\boldsymbol{r}) \psi_\downarrow(\boldsymbol{r}) \psi_\uparrow(\boldsymbol{r}), \tag{6}$$

where $V > 0$ is the coupling constant. A detailed analysis of the relation between the microscopic pairing interaction and the gap symmetry in the band representation can be found in Ref. 23. In particular, in the BCS-contact model (6) the local pairing of electrons with opposite spins translates into the same-helicity pairing, the superconducting gap function has only intraband components, and the order parameter is represented by a single complex function $\eta(\boldsymbol{r})$.

External magnetic field can be included in the electron band theory by making the so-called Peierls substitution[24] in the dispersion functions $\xi_\lambda(\boldsymbol{k})$:

$$\boldsymbol{k} \to \boldsymbol{K} = -i\frac{\partial}{\partial \boldsymbol{r}} + \frac{e}{c}\boldsymbol{A}(\boldsymbol{r}), \tag{7}$$

where $e$ is the absolute value of the electron charge and $\boldsymbol{A}(\boldsymbol{r})$ is the magnetic vector potential. Near the upper critical field, the magnetic induction is uniform, $\boldsymbol{B}(\boldsymbol{r}) = \boldsymbol{H}$, so that $\boldsymbol{A}(\boldsymbol{r}) = (\boldsymbol{H} \times \boldsymbol{r})/2$ in the symmetric gauge. This approach has been used to microscopically derive the Ginzburg-Landau functional for noncentrosymmetric superconductors, both in the clean[14] and disordered[21] cases. However, the bands (4) are nonanalytic in $\boldsymbol{k}$, and the Peierls substitution leads to ill-defined operators. To avoid this, one can make the substitution (7) directly in the original Hamiltonian [Eq. (1)]. Then, the SO coupling, the impurity scattering, and the magnetic field are all incorporated in the following single-electron Hamiltonian in the coordinate-spin representation:

$$\hat{h} = \frac{\boldsymbol{K}^2}{2m^*} + \gamma_0 \boldsymbol{K}\hat{\boldsymbol{\sigma}} + \frac{g}{2}\mu_B \boldsymbol{H}\hat{\boldsymbol{\sigma}} + U(\boldsymbol{r}) - \epsilon_F, \tag{8}$$

where $g$ is the Landé factor, and $\mu_B$ is the Bohr magneton. The final expressions for observable properties, in particular the upper critical field, do not actually depend on whether the Peierls substitution is made in the spin or band representations.

### A. Gap equations

Following the standard textbook procedure, one can calculate the difference between the disorder-averaged free energies in the superconducting and normal states at the same temperature and field. In the vicinity of the upper critical field $H_{c2}(T)$, one can keep only the terms quadratic in the order parameter in the free-energy expansion:

$$\mathcal{F} = \int\int d\boldsymbol{r}_1 d\boldsymbol{r}_2 \eta^*(\boldsymbol{r}_1) S(\boldsymbol{r}_1, \boldsymbol{r}_2) \eta(\boldsymbol{r}_2). \tag{9}$$

We assume that the superconducting phase transition is of second order. It should be noted that the validity of this assumption at all temperatures is not obvious (see, e.g., a discussion in Sec. IV C below) and should be verified by examining the higher-order terms in the free energy, which is beyond the scope of the present work. The kernel in Eq. (9) has the following form:

$$S(\boldsymbol{r}_1, \boldsymbol{r}_2) = \frac{1}{V}\delta(\boldsymbol{r}_1 - \boldsymbol{r}_2) - T{\sum_n}' X(\boldsymbol{r}_1, \boldsymbol{r}_2; \omega_n), \tag{10}$$

where

$$X(\boldsymbol{r}_1, \boldsymbol{r}_2; \omega_n) = \frac{1}{2} g_{\alpha\beta}^\dagger g_{\gamma\delta} \langle G_{\beta\gamma}(\boldsymbol{r}_1, \boldsymbol{r}_2; \omega_n) G_{\alpha\delta}(\boldsymbol{r}_1, \boldsymbol{r}_2; -\omega_n)\rangle_{\mathrm{imp}}, \tag{11}$$

$\omega_n = (2n+1)\pi T$ is the fermionic Matsubara frequency, and $\hat{g} = i\hat{\sigma}_2$. The prime in the second term in Eq. (10) means that the summation is limited to $|\omega_n| \le \omega_c$, where $\omega_c$ is the BCS frequency cutoff. The angular brackets denote the impurity averaging, and $\hat{G}(\boldsymbol{r}_1, \boldsymbol{r}_2; \omega_n)$ is the Matsubara Green's function of electrons in the normal state, which satisfies the equation

$$(i\omega_n - \hat{h}_1)\hat{G}(\boldsymbol{r}_1, \boldsymbol{r}_2; \omega_n) = \delta(\boldsymbol{r}_1 - \boldsymbol{r}_2), \tag{12}$$

with the Hamiltonian $\hat{h}$ given by expression (8). The subscript "1" means that $\hat{h}$ acts on the first argument of the Green's function. The critical temperature at a given field, or inversely the critical field at a given temperature, is found from the condition that the lowest eigenvalue of the operator $\hat{S}$, defined by the kernel (10), is zero.

At zero field, Eq. (12) yields the following expression for the average Green's function:[21]

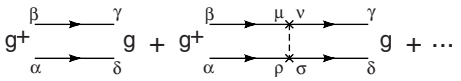


FIG. 1. Impurity ladder diagrams in the Cooper channel. Lines with arrows correspond to the average Green's functions of electrons in the spin representation, $\hat{g}=i\hat{\sigma}_2$, and the impurity (dashed) lines are defined in the text [see Eq. (16)].

$$\hat{G}(\boldsymbol{k},\omega_n)=\sum_{\lambda=\pm}\hat{\Pi}_\lambda(\boldsymbol{k})G_\lambda(\boldsymbol{k},\omega_n), \tag{13}$$

where

$$\hat{\Pi}_\lambda(\mathbf{k})=\frac{1+\lambda\hat{\boldsymbol{k}}\hat{\boldsymbol{\sigma}}}{2} \tag{14}$$

are the band projection operators ($\hat{\boldsymbol{k}}=\boldsymbol{k}/|\boldsymbol{k}|$), and

$$G_\lambda(\boldsymbol{k},\omega_n)=\frac{1}{i\omega_n-\xi_\lambda(\boldsymbol{k})+i\Gamma\ \mathrm{sign}\ \omega_n} \tag{15}$$

are the electron Green's functions in the band representation. Here $\Gamma=1/2\tau$ is the elastic-scattering rate, $\tau=(2\pi n_{\mathrm{imp}}U_0^2N_F)^{-1}$ is the electron mean-free time due to impurities, $N_F=(N_++N_-)/2$, and $N_\lambda$ is the Fermi-level density of states in the $\lambda$th band.

Using the standard techniques,[25] the impurity average of the product of the two Green's functions in Eq. (11) can be represented graphically by ladder diagrams (see Fig. 1) (we assume the disorder that is sufficiently weak for the diagrams with crossed impurity lines to be negligible). Summation of the diagrams is facilitated by representing the impurity line (which corresponds to each "rung" of the ladder) as a sum of spin-singlet and spin-triplet terms:

$$n_{\mathrm{imp}}U_0^2\delta_{\mu\nu}\delta_{\rho\sigma}=\frac{1}{2}n_{\mathrm{imp}}U_0^2g_{\mu\rho}g^\dagger_{\sigma\nu}+\frac{1}{2}n_{\mathrm{imp}}U_0^2\boldsymbol{g}_{\mu\rho}\boldsymbol{g}^\dagger_{\sigma\nu}, \tag{16}$$

where $\hat{\boldsymbol{g}}=i\hat{\boldsymbol{\sigma}}\hat{\sigma}_2$. We introduce an impurity-renormalized gap function $D_{\alpha\beta}(\boldsymbol{q},\omega_n)$, which satisfies an integral equation

$$\begin{aligned}\hat{D}(\boldsymbol{q},\omega_n)=&\ \eta(\boldsymbol{q})\hat{g}+\frac{1}{2}n_{\mathrm{imp}}U_0^2\hat{g}\int\frac{d^3\boldsymbol{k}}{(2\pi)^3}\mathrm{tr}[\hat{g}^\dagger\hat{G}(\boldsymbol{k}+\boldsymbol{q},\omega_n)\\&\times\hat{D}(\boldsymbol{q},\omega_n)\hat{G}^T(-\boldsymbol{k},-\omega_n)]\\&+\frac{1}{2}n_{\mathrm{imp}}U_0^2\hat{\boldsymbol{g}}\int\frac{d^3\boldsymbol{k}}{(2\pi)^3}\mathrm{tr}[\hat{\boldsymbol{g}}^\dagger\hat{G}(\boldsymbol{k}+\boldsymbol{q},\omega_n)\\&\times\hat{D}(\boldsymbol{q},\omega_n)\hat{G}^T(-\boldsymbol{k},-\omega_n)].\end{aligned} \tag{17}$$

Seeking solution in the form

$$\hat{D}(\boldsymbol{q},\omega_n)=d_0(\boldsymbol{q},\omega_n)\hat{g}+\boldsymbol{d}(\boldsymbol{q},\omega_n)\hat{\boldsymbol{g}}, \tag{18}$$

we obtain the following equations for $d_a(\boldsymbol{r},\omega_n)$ ($a=0,1,2,3$):

$$d_a(\boldsymbol{q},\omega_n)=\eta(\boldsymbol{q})\delta_{a0}+\Gamma\sum_{b=0}^{3}\mathcal{Y}_{ab}(\boldsymbol{q},\omega_n)d_b(\boldsymbol{q},\omega_n), \tag{19}$$

where $\eta(\boldsymbol{q})$ is the Fourier transform of the order parameter, and

$$\begin{aligned}\mathcal{Y}_{ab}(\boldsymbol{q},\omega_n)=&\frac{1}{2\pi N_F}\\&\times\int\frac{d^3\boldsymbol{k}}{(2\pi)^3}\mathrm{tr}[\hat{g}_a^\dagger\hat{G}(\boldsymbol{k}+\boldsymbol{q},\omega_n)\hat{g}_b\hat{G}^T(-\boldsymbol{k},-\omega_n)],\end{aligned} \tag{20}$$

with $\hat{g}_0=\hat{g}$, and $\hat{g}_i=\hat{g}_i$ for $i=1,2,3$. We see that, in addition to the spin-singlet component $d_0(\boldsymbol{q},\omega_n)$ of the gap function, impurity scattering can induce a nonzero spin-triplet component $\boldsymbol{d}(\boldsymbol{q},\omega_n)$. Note that the free energy depends only on the singlet component: from Eqs. (11) and (19), we obtain

$$\mathcal{F}=\int\frac{d^3\boldsymbol{q}}{(2\pi)^3}\eta^*(\boldsymbol{q})\left[\frac{1}{V}\eta(\boldsymbol{q})-\pi N_FT\sum_n{}'\frac{d_0(\boldsymbol{q},\omega_n)-\eta(\boldsymbol{q})}{\Gamma}\right]. \tag{21}$$

Substituting the Green's functions (13) into Eq. (20) and calculating the spin traces, we obtain for the singlet-singlet part of the $4\times4$ matrix $\hat{\mathcal{Y}}$:

$$\begin{aligned}\mathcal{Y}_{00}(\boldsymbol{q},\omega_n)=&\frac{1}{2\pi N_F}\sum_\lambda\int\frac{d^3\boldsymbol{k}}{(2\pi)^3}G_\lambda(\boldsymbol{k}+\boldsymbol{q},\omega_n)G_\lambda(-\boldsymbol{k},-\omega_n)\\=&\frac{1}{2}\sum_\lambda\rho_\lambda\left\langle\frac{1}{|\omega_n|+\Gamma+i\Omega\ \mathrm{sign}\ \omega_n}\right\rangle_{\hat{\boldsymbol{k}}}\\=&\left\langle\frac{1}{|\omega_n|+\Gamma+i\Omega\ \mathrm{sign}\ \omega_n}\right\rangle_{\hat{\boldsymbol{k}}},\end{aligned} \tag{22}$$

where

$$\rho_\pm=\frac{N_\pm}{N_F}=1\pm\delta \tag{23}$$

are the fractional densities of states in the two bands, $\Omega(\boldsymbol{k},\boldsymbol{q})=v_F\hat{\boldsymbol{k}}\boldsymbol{q}/2$, and $\langle(\ldots)\rangle_{\hat{\boldsymbol{k}}}$ denotes the averaging over the directions of $\boldsymbol{k}$. The parameter

$$\delta=\frac{N_+-N_-}{N_++N_-}, \tag{24}$$

which characterizes the difference between the band densities of states, can be expressed in terms of the SO coupling strength (3) as follows:

$$|\delta|=\frac{2\varrho\sqrt{1+\varrho^2}}{1+2\varrho^2}. \tag{25}$$

Similarly, for the singlet-triplet mixing part we obtain

$$\begin{aligned}\mathcal{Y}_{0i}(\boldsymbol{q},\omega_n)=&\mathcal{Y}_{i0}(\boldsymbol{q},\omega_n)\\=&\frac{1}{2\pi N_F}\sum_\lambda\lambda\int\frac{d^3\boldsymbol{k}}{(2\pi)^3}\hat{k}_iG_\lambda(\boldsymbol{k}+\boldsymbol{q},\omega_n)G_\lambda(-\boldsymbol{k},-\omega_n)\\=&\delta\left\langle\frac{\hat{k}_i}{|\omega_n|+\Gamma+i\Omega\ \mathrm{sign}\ \omega_n}\right\rangle_{\hat{\boldsymbol{k}}}.\end{aligned} \tag{26}$$

Finally, the triplet-triplet part can be represented as follows:

$$\mathcal{Y}_{ij}(\boldsymbol{q},\omega_n)=\mathcal{Y}_{ij}^{(1)}(\boldsymbol{q},\omega_n)+\mathcal{Y}_{ij}^{(2)}(\boldsymbol{q},\omega_n), \tag{27}$$

where

$$\mathcal{Y}_{ij}^{(1)}(\boldsymbol{q},\omega_n)=\frac{1}{2\pi N_F}\times\sum_{\lambda}\int\frac{d^3\boldsymbol{k}}{(2\pi)^3}\hat{k}_i\hat{k}_j G_\lambda(\boldsymbol{k}+\boldsymbol{q},\omega_n)G_\lambda(-\boldsymbol{k},-\omega_n)=\left\langle\frac{\hat{k}_i\hat{k}_j}{|\omega_n|+\Gamma+i\Omega\ \mathrm{sign}\ \omega_n}\right\rangle_{\hat{\boldsymbol{k}}}, \tag{28}$$

and

$$\mathcal{Y}_{ij}^{(2)}(\boldsymbol{q},\omega_n)=\frac{1}{2\pi N_F}\sum_{\lambda}\int\frac{d^3\boldsymbol{k}}{(2\pi)^3}(\delta_{ij}-\hat{k}_i\hat{k}_j-i\lambda e_{ijl}\hat{k}_l)\times G_\lambda(\boldsymbol{k}+\boldsymbol{q},\omega_n)G_{-\lambda}(-\boldsymbol{k},-\omega_n)=\frac{1}{2}\sum_{\lambda}\left\langle\frac{\delta_{ij}-\hat{k}_i\hat{k}_j-i\lambda e_{ijl}\hat{k}_l}{|\omega_n|+\Gamma+i(\Omega+\lambda E_{\mathrm{SO}}/2)\mathrm{sign}\ \omega_n}\right\rangle_{\hat{\boldsymbol{k}}}. \tag{29}$$

We see that in the band representation the singlet impurity scattering channel, which is described by the first term in Eq. (16), causes only the scattering of intraband pairs between the bands. In contrast, the triplet channel can mix intraband and interband pairs, the latter being described by $\mathcal{Y}_{ij}^{(2)}$.

The interband contribution to $\mathcal{Y}_{ij}$ can be neglected in the limit when the SO coupling is strong compared with both the cut-off energy $\omega_c$ and the elastic-scattering rate $\Gamma$. Setting $\boldsymbol{q}=0$ in Eqs. (28) and (29), we obtain

$$\mathcal{Y}_{ij}^{(1)}(\boldsymbol{0},\omega_n)=\frac{\delta_{ij}}{3(|\omega_n|+\Gamma)}\equiv\mathcal{Y}_{\mathrm{intra}}(\omega_n)\delta_{ij},$$

and

$$\mathcal{Y}_{ij}^{(2)}(\boldsymbol{0},\omega_n)=\frac{2\delta_{ij}}{3(|\omega_n|+\Gamma)(1+r^2)}\equiv\mathcal{Y}_{\mathrm{inter}}(\omega_n)\delta_{ij},$$

where $r(\omega_n)=E_{\mathrm{SO}}/2(|\omega_n|+\Gamma)$. Due to the BCS cutoff, the maximum value of $\omega_n$ is equal to $\omega_c$; therefore $r_{\min}\sim E_{\mathrm{SO}}/\max(\omega_c,\Gamma)\gg 1$. From this it follows that

$$\max_n\frac{\mathcal{Y}_{\mathrm{inter}}(\omega_n)}{\mathcal{Y}_{\mathrm{intra}}(\omega_n)}=\frac{2}{1+r_{\min}^2}\sim\left[\frac{\max(\omega_c,\Gamma)}{E_{\mathrm{SO}}}\right]^2\ll 1.$$

Therefore the interband contribution is small compared with the intraband one at all Matsubara frequencies.

The superconducting critical temperature is found by setting $\boldsymbol{q}=0$, then $\mathcal{Y}_{0i}=\mathcal{Y}_{i0}=0$, and the solution of Eq. (19) has the form $d_0=(1+\Gamma/|\omega_n|)\eta$. Substituting this into Eq. (21) and comparing the result with Eq. (9), we obtain

$$S(\boldsymbol{q}=0)=\frac{1}{V}-\pi N_F T\sum_n{}'\frac{1}{|\omega_n|}, \tag{30}$$

which yields the superconducting critical temperature:

$$T_{c0}=\frac{2e^{\mathbb{C}}}{\pi}\omega_c e^{-1/N_F V}, \tag{31}$$

where $\mathbb{C}\simeq 0.577$ is Euler's constant. Thus there is an analog of Anderson's theorem in noncentrosymmetric superconductors with a BCS-contact pairing interaction: The zero-field critical temperature is not affected by scalar disorder.[21]

Now let us turn on a uniform magnetic field $\boldsymbol{H}=H\hat{z}$. Its orbital effect is taken into account in the usual way by replacing $\boldsymbol{q}\to\boldsymbol{D}=-i\boldsymbol{\nabla}+(2e/c)\boldsymbol{A}$ in $\mathcal{Y}_{ab}(\boldsymbol{q},\omega_n)$, which become differential operators of infinite order. The gap equations [Eq. (19)] then take the following form:

$$(1-\Gamma\hat{\mathcal{Y}}_{00})d_0-\Gamma\hat{\mathcal{Y}}_{0i}d_i=\eta,$$

$$-\Gamma\hat{\mathcal{Y}}_{i0}d_0+(\delta_{ij}-\Gamma\hat{\mathcal{Y}}_{ij})d_j=0. \tag{32}$$

Solution of these equations in the general case is rather cumbersome. In order to make progress, we use the fact that in practice the SO coupling is much weaker than the Fermi energy. In terms of the parameter $\delta$, this translates into the following condition: $|\delta|\ll 1$. This allows us to neglect the triplet component of the gap function. Indeed, using the fact that the singlet-triplet mixing is described by $\mathcal{Y}_{0i}=\mathcal{Y}_{i0}$, which are proportional to $\delta$ [see Eq. (26)], one can solve the gap equations by iterations. It is easy to see that $\boldsymbol{d}\sim\mathcal{O}(\delta)$; therefore the correction to $d_0=(1-\Gamma\hat{\mathcal{Y}}_{00})^{-1}\eta$ due to the impurity-induced singlet-triplet mixing is of the order of $\delta^2$ and will be neglected.

### B. Equation for $H_{c2}(T)$

Keeping only the singlet gap component, we have $d_0=(1-\Gamma\hat{\mathcal{Y}}_{00})^{-1}\eta$. Substituting this in Eq. (21), we can represent the operator $\hat{S}$ as follows:

$$\hat{S}=\frac{1}{V}-\pi N_F T\sum_n{}'[1-\Gamma\hat{\mathcal{Y}}_{00}(\omega_n)]^{-1}\hat{\mathcal{Y}}_{00}(\omega_n), \tag{33}$$

where $\hat{\mathcal{Y}}_{00}(\omega_n)$ is defined by the kernel

$$\mathcal{Y}_{00}(\boldsymbol{r}_1,\boldsymbol{r}_2;\omega_n)=\frac{1}{2\pi N_F}g_{\alpha\beta}^{\dagger}g_{\gamma\delta}\times\langle G_{\beta\gamma}(\boldsymbol{r}_1,\boldsymbol{r}_2;\omega_n)\rangle_{\mathrm{imp}}\langle G_{\alpha\delta}(\boldsymbol{r}_1,\boldsymbol{r}_2;-\omega_n)\rangle_{\mathrm{imp}}. \tag{34}$$

Although the expression (33) is approximate (with the corrections of the order of $\delta^2$), it has the advantage of being relatively simple and captures important physics of the problem, including the properties of various nonuniform superconducting states created by the external field (see Secs. III–V below). The case of arbitrary SO coupling, with both singlet and triplet channels present but without paramagnetic effects, is considered in Ref. 26.

It is shown in the Appendix that the eigenfunctions of $\hat{\mathcal{Y}}_{00}(\omega_n)$ are the Landau levels $|N,p\rangle$, which are labeled by two quantum numbers: a non-negative integer $N$ and a real $p$. The latter is proportional to the wave vector of the order-

parameter modulation along the applied field: $p=\ell_H q_z$, where $\ell_H=\sqrt{c/eH}$ is the magnetic length. The corresponding eigenvalues can be written as follows:

$$\hat{\mathcal{Y}}_{00}(\omega_n)|N,p\rangle = y_{N,p}(\omega_n)|N,p\rangle, \tag{35}$$

where

$$y_{N,p}(\omega_n) = \int_0^\infty du e^{-(|\omega_n|+\Gamma)u} \times \int_0^1 ds F_p(u,s) e^{-v^2(1-s^2)/2} L_N[v^2(1-s^2)]. \tag{36}$$

Here $v=(v_F/2\ell_H)u$, $L_N(x)$ are the Laguerre polynomials,

$$F_p(u,s) = \cos(p_0 vs)\cos(pvs) - \delta \sin(p_0 vs)\sin(pvs), \tag{37}$$

$p_0=g\mu_B H\ell_H/v_F$, and $\delta$ is defined by Eq. (24). Note that, in *centrosymmetric* isotropic superconductors with nonmagnetic impurities, the eigenvalues of $\hat{\mathcal{Y}}_{00}(\omega_n)$ are given by the same expression (36) but with $F_p(u,s)=\cos(p_0 v)\cos(pvs)$. This is still different from Eq. (37), even if one sets $\delta=0$ in the latter. The reason is that Eq. (37) is valid under the assumption that the Zeeman energy is small compared with the SO band splitting.

Since the Landau levels are eigenfunctions of $\hat{\mathcal{Y}}_{00}(\omega_n)$ at all frequencies, the operator $\hat{S}$ [see Eq. (33)] is also diagonal in the basis of $|N,p\rangle$. Using Eqs. (30) and (31), we can eliminate both the frequency cutoff and the coupling constant from Eq. (33). In this way we obtain an equation for the magnetic field at which a superconducting instability characterized by $N$ and $p$ develops:

$$\ln\frac{T_{c0}}{T} = \pi T \sum_n \left[\frac{1}{|\omega_n|} - \frac{y_{N,p}(\omega_n)}{1-\Gamma y_{N,p}(\omega_n)}\right]. \tag{38}$$

The upper critical field, $H_{c2}(T)$, is obtained by maximizing the solution of the above equation with respect to both $N$ and $p$.

It is convenient to introduce the reduced temperature, magnetic field, and disorder as follows:

$$t=\frac{T}{T_{c0}}, \quad h=\frac{2H}{H_0}, \quad \zeta=\frac{\Gamma}{\pi T_{c0}}, \tag{39}$$

where $H_0=\Phi_0/\pi\xi_0^2$, $\Phi_0=\pi c/e$ is the magnetic-flux quantum, and $\xi_0=v_F/2\pi T_{c0}$ is the superconducting coherence length. Equation (38) then takes the form

$$\ln\frac{1}{t} = 2\sum_{n\geq 0}\left[\frac{1}{2n+1} - t\frac{w_n^{(N,Q)}(t,h)}{1-\zeta w_n^{(N,Q)}(t,h)}\right], \tag{40}$$

where

$$w_n^{(N,Q)}(t,h) = \int_0^\infty d\rho e^{-[(2n+1)t+\zeta]\rho} \int_0^1 ds \Phi_Q(\rho,s) \times \exp\left[-\frac{h}{4}\rho^2(1-s^2)\right] L_N\left[\frac{h}{2}\rho^2(1-s^2)\right], \tag{41}$$

and

$$\Phi_Q(\rho,s) = \cos(\alpha h\rho s)\cos(Q\rho s) - \delta\sin(\alpha h\rho s)\sin(Q\rho s). \tag{42}$$

The parameter

$$\alpha = \frac{g}{2}\frac{\mu_B H_0}{2\pi T_{c0}} \tag{43}$$

measures the relative importance of the paramagnetic and orbital contributions to the magnetic suppression of superconductivity (note that $\alpha$ is proportional to the Maki parameter $\alpha_M$, introduced in Ref. 27). For the upper critical field in the reduced notations, we have

$$h_{c2}(t) = \max_{N,Q} h_{N,Q}(t), \tag{44}$$

where $h_{N,Q}(t)$ is the solution of Eq. (40), $N$ is the Landau-level index, and $Q=\xi_0 q_z$ is the dimensionless wave vector of the superconducting instability.

The purely orbital limit is obtained by formally setting $g$ to zero. Then $\alpha=0$, and Eq. (40) takes exactly the same form as in centrosymmetric BCS superconductors. Therefore, if the Zeeman interaction is neglected then the absence of inversion symmetry in the weak SO coupling limit does not bring about any new features in $H_{c2}(T)$, compared with the centrosymmetric case, which is described by the Helfand-Werthamer theory.[16] The maximum critical field corresponds to $N=Q=0$ at all temperatures. In particular, at $T=0$ and in the absence of impurities one obtains: $H_{c2}(0)=(e^{2-C}/8)H_0 \simeq 0.52H_0$. This can be used to relate $\alpha$ to experimentally observable quantities as follows:

$$\alpha \simeq 0.21\frac{H_{c2}(0)[T]}{T_{c0}[K]}. \tag{45}$$

Here we assumed $g=2$.

## III. GINZBURG-LANDAU REGIME

At weak external field, the critical temperature is close to $T_{c0}$, i.e., the reduced temperature $t$ is close to one. In this limit, one can solve Eq. (40) analytically by expanding $w_n^{(N,Q)}$ in powers of $h$ and $Q$ (we set $N=0$). We seek solution in the form

$$t_c(h) = 1 - a_1 h - a_2 h^2 + \mathcal{O}(h^3). \tag{46}$$

It follows from Eq. (42) that the maximum critical temperature corresponds to

$$Q = -\delta\alpha h. \tag{47}$$

After some straightforward algebra, we obtain the following expressions for the coefficients in the expansion (46):

$$a_1 = \frac{1}{3}\mathcal{S}_{2,1}, \tag{48}$$

$$a_2 = \frac{1}{18}\mathcal{S}_{2,1}^2 + \frac{1}{9}\mathcal{S}_{2,1}\mathcal{S}_{1,2} - \frac{2}{5}\mathcal{S}_{2,3} - \frac{1}{9}\zeta\mathcal{S}_{3,3} + \frac{1}{3}\alpha^2\mathcal{S}_{2,1}, \tag{49}$$

with

$$\mathcal{S}_{k,l}(\zeta) = 2\sum_{n\geq 0}\frac{1}{(2n+1)^k(2n+1+\zeta)^l}.$$

Since our model is valid only in the limit of weak SO coupling, $|\delta| \ll 1$, we have omitted in these expressions the terms containing $\delta^2$. In the clean limit, we have

$$a_1 = \frac{7\zeta(3)}{12},$$

$$a_2 = \frac{49\zeta^2(3)}{96} - \frac{31\zeta(5)}{40} + \frac{7\zeta(3)}{12}\alpha^2,$$

where $\zeta(x)$ is the Riemann zeta function.

Since Eq. (48) does not contain $\alpha$, the slope of the upper critical field near $T_{c0}$ is entirely determined by the orbital effects. Returning to dimensional variables, we obtain

$$\left|\frac{dH_{c2}}{dT}\right|_{T=T_{c0}} = \frac{6\pi}{\mathcal{S}_{2,1}(\zeta)}\frac{\Phi_0 T_{c0}}{v_F^2}, \tag{50}$$

which has exactly the same form as in isotropic centrosymmetric superconductors.[28] From this expression it follows that, in particular, the upper critical-field slope in our model is enhanced by disorder, in agreement with the results obtained in Ref. 21.

The effects of the Zeeman interaction on the critical temperature appear only in the second order in $h$ and are described by the last term in Eq. (49). If the difference between the band densities of states is taken into account (i.e., if $\delta \neq 0$), then the order parameter is modulated along the applied field, with the period given by Eq. (47).

In the limit of large $\alpha$, the Zeeman term dominates and the critical-field slope diverges: $H_{c2}(T) \sim \sqrt{T_{c0}-T}$. Similar to the orbital critical field (50), the paramagnetic critical field in the Ginzburg-Landau regime is enhanced by disorder. The paramagnetic pair breaking in noncentrosymmetric superconductors has some peculiar features, compared with the centrosymmetric case, and is studied in detail in the next section.

## IV. PARAMAGNETIC LIMIT

The purely paramagnetic limit corresponds to $\alpha \to \infty$ in Eq. (40). Due to the fast oscillations of $\Phi_Q$, the last two factors in the $s$ integral in Eq. (41) can be replaced by one, and the solution becomes degenerate with respect to $N$. We have

$$w_n(Q) = \frac{1}{2}\sum_\lambda \rho_\lambda \mathrm{Re}\left\langle \frac{1}{(2n+1)t + \zeta + i(Q+\lambda\tilde{h})\hat{k}_z}\right\rangle_{\hat{\mathbf{k}}}, \tag{51}$$

where

$$\tilde{h} = \frac{g}{2}\frac{\mu_B H}{\pi T_{c0}} = \alpha h. \tag{52}$$

Calculating the Fermi-surface integrals, we obtain

$$w_n(Q) = \frac{1}{2}\sum_\lambda \rho_\lambda \frac{1}{Q+\lambda\tilde{h}}\arctan\frac{Q+\lambda\tilde{h}}{(2n+1)t+\zeta}. \tag{53}$$

Further analytical progress can be made in two limiting cases: clean ($\zeta=0$) and "dirty" ($\zeta \gg 1$), while the intermediate disorder strengths can only be studied numerically.

### A. Clean case

In the clean limit, it is convenient to go back to expression (51) and substitute it into Eq. (40), with the following result:

$$\ln\frac{1}{t} = \frac{1}{2}\sum_\lambda \rho_\lambda \left\langle \mathrm{Re}\,\Psi\left(\frac{1}{2} + i\frac{Q+\lambda\tilde{h}}{2t}\hat{k}_z\right)\right\rangle_{\hat{\mathbf{k}}} - \Psi\left(\frac{1}{2}\right), \tag{54}$$

where $\Psi(x)$ is the digamma function. From this we obtain

$$t = \exp[\max_y \mathcal{I}(y,z)], \tag{55}$$

where $y=Q/2t$, $z=\tilde{h}/2t$,

$$\mathcal{I}(y,z) = \Psi\left(\frac{1}{2}\right) - \frac{1}{2}\sum_\lambda \rho_\lambda \frac{\mathrm{Im}\ln\Gamma(1/2 + iy + i\lambda z)}{y+\lambda z},$$

and $\Gamma(x)$ is the gamma function. At any given $z$, if the maximum of $\mathcal{I}(y,z)$ is achieved at $y=y_c$, then the wave vector of the superconducting instability is $Q=2ty_c$, and the corresponding critical field is $\tilde{h}=2tz$. The critical field of a second-order phase transition into a uniform superconducting state can be found by setting $y=0$ in Eq. (55). In particular, at zero temperature this phase transition occurs at $\tilde{h}_0 = 1/2e^{C-1} \simeq 0.76$.

The pair-breaking effect of the Zeeman interaction can be reduced by allowing the pairs to have a nonzero center-of-mass momentum. The outcome of the competition between the Zeeman energy and the gradient energy depends on the difference between the densities of states in the two bands, which in turn depends on the ratio of the SO band splitting to the Fermi energy [see Eqs. (23) and (25)]. If it is neglected, i.e., $\delta=0$, then one obtains from Eq. (55) that at $z<z^* \simeq 0.44$, which corresponds to high temperatures, $t>t^* \simeq 0.68$, and low fields, $\tilde{h}<\tilde{h}^* \simeq 0.60$, the maximum critical field is achieved at $Q=0$, and the phase transition occurs into the uniform superconducting state. However, at $t<t^*$ the maximum critical field corresponds to $Q \neq 0$, and the phase transition occurs into a nonuniform superconducting state

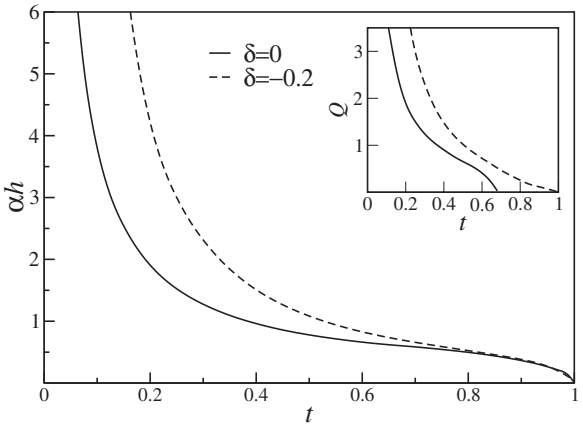


FIG. 2. Paramagnetic critical field $\tilde{h}=\alpha h$ in the clean case for the LOFF state ($\delta=0$) and the helical state with $\delta=-0.2$. The inset shows the temperature dependence of the wave vector $Q$ of the order-parameter modulation along the field.

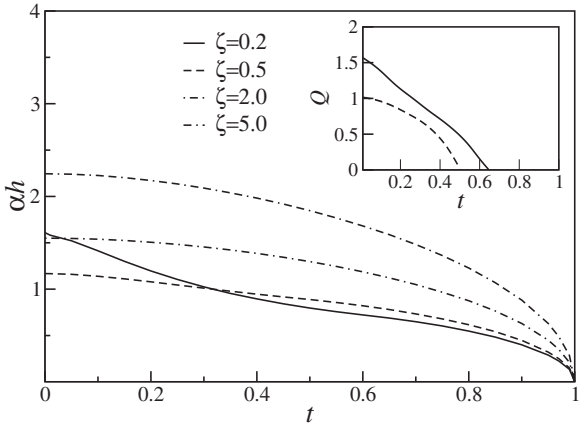


FIG. 3. Paramagnetic critical field in the LOFF state ($\delta=0$) for different strengths of disorder: $\zeta=0.2$, 0.5, 2.0, and 5.0 from bottom to top. The inset shows the order-parameter modulation along the field (for $\zeta=2.0$ and 5.0, $Q=0$ at all temperatures).

similar to the Larkin-Ovchinnikov-Fulde-Ferrell (LOFF) state.[29] The order parameter is modulated along the field: $\eta(\boldsymbol{r})=\eta_1 e^{iqz}+\eta_2 e^{-iqz}$, where $q=Q/\xi_0$. The coefficients $\eta_{1,2}$ are found from the higher-order terms in the free energy. In Refs. 20 and 30 this was done for a Rashba superconductor, and it was shown that both a multiple-$q$ (or stripe) LOFF state and a single plane-wave state are possible, depending on temperature.

If the difference between $\rho_+$ and $\rho_-$ is taken into account, then the right-hand side of Eq. (54) is no longer even in $Q$, and the maximum critical field corresponds to $Q\neq 0$ at all temperatures $0\leq t<1$. In this case, the phase transition occurs into a single plane-wave, or helical,[13] superconducting state with $\eta(\boldsymbol{r})=\eta_0 e^{iqz}$. In particular, at weak fields near $t=1$, the maximum of $\mathcal{I}(y,z)$ is achieved at $y_c=-\delta z$, which corresponds to $Q=-\delta\tilde{h}$. For the critical-field one obtains

$$\tilde{h}|_{t\to 1}=\sqrt{\frac{12}{7\zeta(3)}}(1-t)^{1/2}. \tag{56}$$

At low temperatures, we use the fact that $\max_y \mathcal{I}(y,z)=-(\rho_+/2)\ln(8e^{\mathbb{C}-1}z)$ in the limit $z\to\infty$ (for $\rho_+\leq\rho_-$). Therefore,

$$\tilde{h}|_{t\to 0}=\frac{1}{4e^{\mathbb{C}-1}}t^{-\rho_-/\rho_+}. \tag{57}$$

In these expressions we have omitted the terms proportional to $\delta^2$. The temperature dependence of the critical field is shown in Fig. 2, both in the LOFF state, for $\rho_+=\rho_-=1$, and in the helical state, for $\rho_+=0.8$ and $\rho_-=1.2$.

The most notable feature of the phase diagram is a considerable weakening of the paramagnetic pair breaking at low temperatures, which is manifested in the divergence of the critical field at $t\to 0$.[31] Similar behavior has also been found in two-dimensional noncentrosymmetric superconductors.[19,20]

We would like to mention that the paramagnetic pair breaking disappears altogether in the (rather unrealistic) extreme single-band case $|\delta|=1$, which corresponds to a very strong SO coupling, $\varrho\to\infty$ [see Eq. (25)]. Although a quantitative treatment of this case is beyond the limits of applicability of our model, one can use simple arguments to show that the critical temperature is not affected by the applied field. We first note that the Zeeman interaction causes an anisotropic deformation of the electron bands: $\xi_\lambda(\boldsymbol{k})\to\xi_\lambda(\boldsymbol{k})+\lambda(g/2)\mu_B\hat{\boldsymbol{k}}\boldsymbol{H}$. The intraband pairing of electrons with opposite momenta costs additional energy at $H\neq 0$, resulting in the uniform superconductivity being suppressed by the Zeeman field. On the other hand, it is easy to see that the field-induced deformation of the bands amounts to shifting the bands in the opposite directions along the field: $\xi_\lambda(\boldsymbol{k})\to\xi_\lambda(\boldsymbol{k}+\boldsymbol{q}_\lambda)$, where $\boldsymbol{q}_\lambda=\lambda(g/2)\mu_B\boldsymbol{H}/v_F$. If the Cooper pairs in the "+" and "−" bands are completely decoupled, or if there is just one band present, then the band shifts can be eliminated by independent gauge transformations, and the Zeeman pair breaking will be absent. According to Ref. 23, in the BCS-contact model (6) the pairs in the two bands are in fact strongly coupled so that both condensates are characterized by the same wave function $\eta(\boldsymbol{r})$. The band shifts cannot be eliminated simultaneously in both bands by any gauge transformation. Therefore, in general there is some energy penalty associated with the Cooper pairing (both uniform and nonuniform) at $H\neq 0$, compared with the zero-field case.

### B. Disordered case

At arbitrary disorder, the paramagnetic critical field is obtained by numerical solution of Eq. (40), with $w_n$ given by expression (53). At $\delta=0$, we find that the LOFF modulation is suppressed by impurities (see Fig. 3) and disappears at $\zeta>\zeta_c\simeq 1.16$. In contrast, the helical modulation at $\delta\neq 0$ survives even if the impurity scattering is strong, as shown in Fig. 4. In both cases, the low-temperature divergence of the critical-field characteristic of a clean system [see Eq. (57)] is removed by disorder.

In the dirty limit $\zeta\gg 1$, one can obtain an equation for the critical field in a closed form. We shall see that both $Q$ and $\tilde{h}$ scale as $\sqrt{\zeta}\ll\zeta$. Therefore, one can perform the Taylor expansion in Eq. (53):

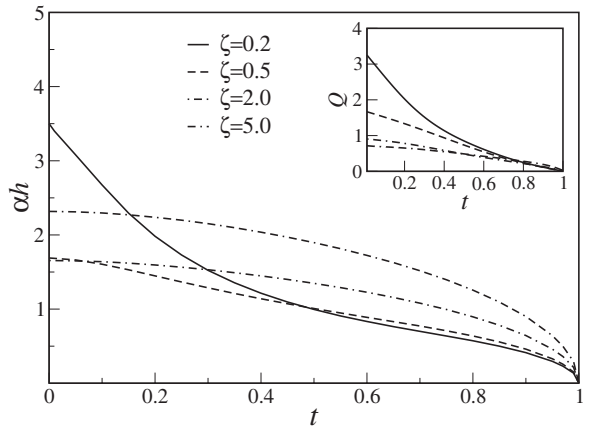


FIG. 4. Paramagnetic critical field in the helical state with $\delta=-0.2$ for different strengths of disorder: $\zeta=0.2$, 0.5, 2.0, and 5.0 from bottom to top. The inset shows the order-parameter modulation along the field.

$$w_n(Q) \simeq \frac{1}{(2n+1)t+\zeta}\left\{1-\frac{W}{[(2n+1)t+\zeta]^2}\right\},$$

where $W=(Q^2+\tilde{h}^2+2\delta Q\tilde{h})/3$. The main contribution to the Matsubara sum in Eq. (40) comes from $(2n+1)t \ll \zeta$, and we obtain $\ln(1/t)=\Psi(1/2+W/2\zeta t)-\Psi(1/2)$. It is easy to see that the maximum critical temperature is achieved when $W$ has a minimum with respect to $Q$, which happens for $Q=-\delta\tilde{h}$, at all temperatures. Thus we arrive at a well-known universal equation, which describes magnetic pair breaking in superconductors:[32]

$$\ln\frac{1}{t}=\Psi\left(\frac{1}{2}+\frac{\sigma}{t}\right)-\Psi\left(\frac{1}{2}\right). \tag{58}$$

The pair-breaker strength is characterized by $\sigma=\tilde{h}^2/6\zeta$. Analytical expressions for the critical field can be obtained in the weak-field limit:

$$\tilde{h}|_{t\to 1}=\sqrt{\frac{12\zeta}{\pi^2}}(1-t)^{1/2}, \tag{59}$$

and also at low temperatures:

$$\tilde{h}|_{t\to 0}=\sqrt{\frac{3\zeta}{2e^{\mathrm{C}}}}. \tag{60}$$

Thus we come to the conclusion that, while the critical field near $T_{c0}$ is enhanced by disorder, the impurity response at low temperatures is nonmonotonic: initially, the disorder cuts off the singularity at $T\to 0$, thus reducing the critical field. However, as the disorder increases one eventually reaches the universal regime, in which the critical field grows as $\sqrt{\zeta}$.

### C. First-order phase transition

Let us now compare the paramagnetic critical fields found above with the critical field of a first-order phase transition (FOPT) into a uniform superconducting state at zero temperature. For simplicity, we neglect the difference between the band densities of states and set $g=2$. Following the arguments of Clogston and Chandrasekhar,[33] we obtain $\mu_B H_{\mathrm{FOPT}}=(\eta_0/\sqrt{2})(1-\chi_s/\chi_P)^{-1/2}$, where $\eta_0=(\pi/e^{\mathrm{C}})T_{c0}$ is the gap magnitude at zero temperature and field, $\chi_s$ is the residual susceptibility at $T=0$ in the superconducting state, and $\chi_P=2\mu_B^2 N_F$ is the Pauli susceptibility in the normal state. Therefore,

$$\tilde{h}_{\mathrm{FOPT}}|_{t\to 0}=\frac{1}{\sqrt{2e^{\mathrm{C}}}}\left(1-\frac{\chi_s}{\chi_P}\right)^{-1/2}. \tag{61}$$

According to Ref. 9, the residual susceptibility in our model is given by the following expression:

$$\frac{\chi_s}{\chi_P}=\frac{2}{3}+\frac{1}{3}\Phi(x), \tag{62}$$

where $x=2\Gamma/3\eta_0$, and

$$\Phi(x)=1-\frac{\pi}{2x}\left(1-\frac{4}{\pi\sqrt{1-x^2}}\arctan\sqrt{\frac{1-x}{1+x}}\right)$$

[at $x>1$ this function is evaluated using $\arctan(ix)=i\tanh^{-1}(x)$]. In the clean limit, $\Phi(0)=0$ and $\chi_s/\chi_P=2/3$. Therefore, $\tilde{h}_{\mathrm{FOPT}}=\sqrt{3/2}e^{-\mathrm{C}}\simeq 0.69$, which is much lower than the divergent expression (57). In the dirty limit $x\to\infty$, we have $\Phi(x)\simeq 1-\pi/2x$, and it follows from Eq. (61) that $\tilde{h}_{\mathrm{FOPT}}=\sqrt{2\zeta/\pi e^{\mathrm{C}}}$. Although the critical field of the first-order phase transition into a uniform superconducting state increases with disorder, it remains lower than the critical field of the second-order phase transition into the helical state, which is given by expression (60).

## V. GENERAL CASE: ORBITAL EFFECTS

Solution of Eq. (40) at all temperatures and for arbitrary values of $\alpha$ and $\zeta$ can only be obtained numerically. To facilitate numerical analysis, we represent the integrals in Eq. (41) in a somewhat shorter form by introducing the Cartesian coordinates $\boldsymbol{\rho}=(\rho_1,\rho_2,\rho_3)$, such that $\rho=|\boldsymbol{\rho}|$, $\rho s=\rho_3$, and $\rho^2(1-s^2)=\rho_\perp^2=\rho_1^2+\rho_2^2$. Using the Fourier transform,

$$\int d^3\boldsymbol{\rho}\, e^{i\mathbf{k}\boldsymbol{\rho}}\frac{e^{-a\rho}}{\rho^2}=\frac{4\pi}{k}\arctan\frac{k}{a},$$

we obtain

$$w_n^{(N,Q)}(t,h)=\frac{1}{2}\sum_\lambda \rho_\lambda\int_0^\infty \frac{kdk}{\sqrt{k^2+(Q+\lambda\alpha h)^2}} \times\arctan\left[\frac{\sqrt{k^2+(Q+\lambda\alpha h)^2}}{(2n+1)t+\zeta}\right]I_N(k), \tag{63}$$

where

$$I_N=\frac{1}{2\pi}\int d^2\boldsymbol{\rho}_\perp e^{-i\mathbf{k}\boldsymbol{\rho}_\perp}e^{-h\rho_\perp^2/4}L_N\left(\frac{h\rho_\perp^2}{2}\right). \tag{64}$$

In the purely paramagnetic limit, $I_N=2\pi\delta(\mathbf{k})$, and one recovers Eq. (53).

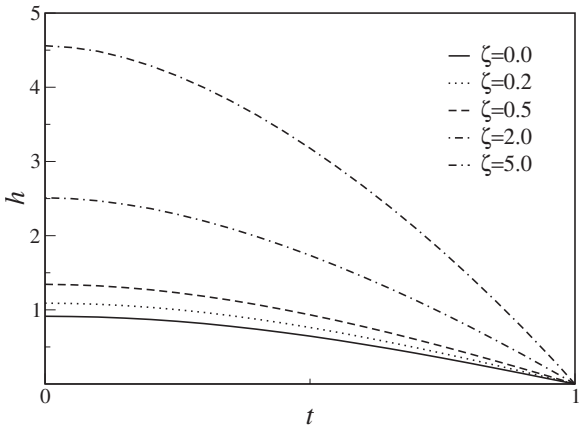


FIG. 5. Upper critical field $h_{c2}(t)$ in the helical vortex state with $\alpha=0.2$ and $\delta=-0.2$ for different strengths of disorder: $\zeta=0.0$, 0.2, 0.5, 2.0, and 5.0 from bottom to top.

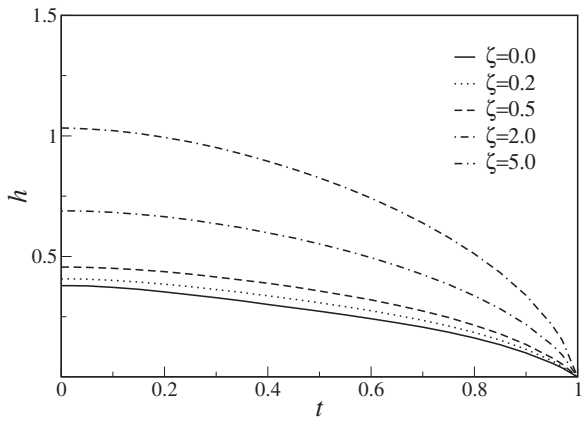


FIG. 6. Upper critical field $h_{c2}(t)$ in the helical vortex state with $\alpha=2.0$ and $\delta=-0.2$ for different strengths of disorder: $\zeta=0.0$, 0.2, 0.5, 2.0, and 5.0 from bottom to top.

The maximum critical field corresponds to $N=0$, in which case $I_0(k)=(2/h)\exp(-k^2/h)$. The order parameter is nonuniform along the direction of the applied field while its dependence on the transverse coordinates is given by the usual Abrikosov vortex solution. As in the purely paramagnetic limit, the phase diagram turns out to be different for $\delta=0$ (LOFF vortex state) and $\delta\neq 0$ (helical vortex state).

Solution of Eqs. (40) and (63) shows that the LOFF state is suppressed by the orbital effects even in the clean case. There is a critical strength of the paramagnetic interaction, $\alpha_c$, below which the LOFF state disappears, i.e., $Q=0$ at all temperatures (in the clean limit $\alpha_c\simeq 0.66$). This is qualitatively similar to the way the orbital interaction affects the LOFF state in centrosymmetric superconductors (see Ref. 34). In contrast, the helical modulation at $\delta\neq 0$, albeit weakened by the orbital effects, does not completely disappear until $\alpha=0$.

In order to study the combined effect of the orbital interaction and impurities, we focus on the helical vortex state with $\delta=-0.2$. We consider $\alpha=0.2$ [which is close to the estimates for the $Li_2(Pd_{1-x},Pt_x)_3B$ family of superconductors, as obtained from Eq. (45) using the data from Ref. 38] and also $\alpha=2.0$. The upper critical-field curves for a range of disorder strengths are shown in Figs. 5 and 6. We see that, if $\alpha$ is not too large, disorder produces a monotonic enhancement of $H_{c2}$ at all temperatures.

In the dirty limit, it is again possible to obtain a relatively simple equation for the upper critical field. Repeating the arguments from Sec. IV B, one can show that the equation has the universal form (58), with the paramagnetic and orbital interactions both contributing to the pair-breaking strength:

$$\sigma=\frac{h+\alpha^2h^2}{6\zeta}. \tag{65}$$

The maximum critical field is achieved for $Q=-\delta\alpha h$. Near $T_{c0}$, superconductivity is suppressed by magnetic field according to Eq. (46), in which $a_1=\pi^2/12\zeta+O(\zeta^{-2})$ and $a_2=(\pi^2/12\zeta)\alpha^2+O(\zeta^{-2})$. At low temperatures, returning to dimensional variables, we arrive at the following expression for the upper critical field:

$$H_{c2}(0)=\frac{\Phi_0}{2\pi\xi_0^2}\frac{1}{2\alpha^2}\left(\sqrt{1+\frac{6\alpha^2}{\pi e^{\mathrm{C}}}\frac{\Gamma}{T_{c0}}}-1\right). \tag{66}$$

In the weak SO coupling limit, corrections to this expression are of the order of $\delta^2$. In the orbital limit $\alpha\to 0$, one obtains $H_{c2}(0)=(3\Gamma/2\pi e^{\mathrm{C}}T_{c0})(\Phi_0/2\pi\xi_0^2)$, while in the paramagnetic limit $\alpha\to\infty$, Eq. (60) is recovered. We see that the upper critical field is enhanced by disorder.

As for the wave vector of the helical modulation, expression (47) is exact only in the Ginzburg-Landau regime and in the dirty limit. In clean systems at low temperatures, deviations of $Q/(-\delta\alpha h)$ from unity become quite substantial [see Fig. 7].

## VI. CONCLUSIONS

We have calculated the upper critical field in noncentrosymmetric superconductors at arbitrary temperatures, both in the clean case and in the presence of scalar impurities,

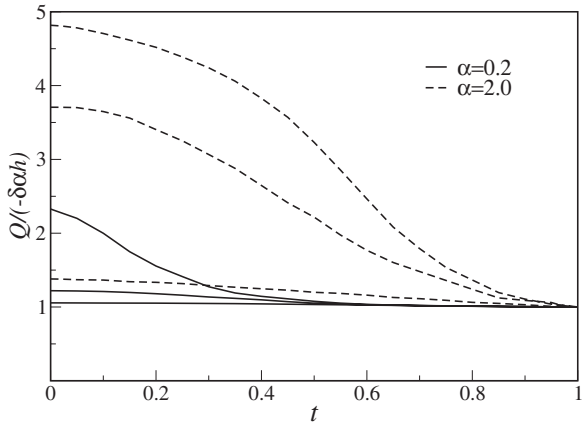


FIG. 7. Ratio $Q/(-\delta\alpha h)$ in the helical vortex state with $\delta=-0.2$ for the following disorder strengths: $\zeta=0.0$, 0.5, and 5.0 (from top to bottom).

using as an example a crystal of cubic symmetry with a BCS-contact pairing interaction. Our derivation relies on the assumption that the SO band splitting is small compared to the Fermi energy. In this case, one can neglect the disorder-induced triplet component of the gap function, which considerably simplifies the calculations, without losing information about the interesting physics of the problem, in particular about the properties of nonuniform superconducting states.

As in the centrosymmetric case, the pair breaking is provided by both the orbital and the Zeeman (paramagnetic) interactions. If the former is dominant, i.e., $\alpha \to 0$ [see Eqs. (43) and (45)], then the lack of inversion symmetry in the weak SO coupling limit does not have any appreciable effect on the upper critical field, which is described by the standard Helfand-Werthamer theory. However, as $\alpha$ increases, so do the deviations from the centrosymmetric case. In the extreme paramagnetic limit, corresponding to $\alpha \to \infty$, the critical field diverges at $T \to 0$ in the clean case.

Impurities suppress both the orbital and paramagnetic pair breakings [see Eqs. (58) and (65)], resulting in an enhancement of the upper critical field. In the strongly paramagnetic limit, the effects of disorder on the low-temperature critical field are nonmonotonic: at weak disorder $H_{c2}$ decreases but in the dirty limit the overall enhancement of the critical field takes over.

The spatial structure of the superconducting order parameter is, in general, different from the centrosymmetric case. As soon as the difference between the densities of states in the SO-split bands, $N_+$ and $N_-$, is taken into account, the system exhibits a helical instability, in which the order parameter has a phase gradient along the applied magnetic field (in a cubic crystal). The helical superconducting state turns out to be robust with respect to both the orbital pair breaking and disorder. In particular, the wave vector of the superconducting instability in the Ginzburg-Landau regime and in the dirty limit is given by $q_z = -2\delta\alpha(H/H_0)\xi_0^{-1}$. In contrast, the LOFF state, which occupies the low-temperature part of the phase diagram at $N_+ = N_-$, is quickly suppressed by both the orbital interaction and disorder similarly to its counterpart in the centrosymmetric case.[34,35]

Let us discuss the application of our results to the family of cubic noncentrosymmetric compounds $Li_2(Pd_{1-x},Pt_x)_3B$, where $x$ ranges from zero to one. The critical temperature varies from 7–8 K for $x=0$ to 2.2–2.8 K for $x=1$. The electronic band structure also exhibits considerable variation: the SO band splitting is strongly anisotropic, and can be as large as 30 meV in $Li_2Pd_3B$ and 200 meV in $Li_2Pt_3B$ (Ref. 36). Experimental data[37,38] seem to agree that $Li_2Pd_3B$ is a conventional BCS-like superconductor with no gap nodes. In contrast, the gap structure in $Li_2Pt_3B$ is still a subject of controversy. While earlier experiments (see Ref. 37) suggested the presence of lines of nodes in the gap, the recent $\mu$SR and specific-heat data[38] have found no evidence of those. Moreover, according to Ref. 38, the whole $Li_2(Pd_{1-x},Pt_x)_3B$ family of compounds are single-gap isotropic superconductors. If this is the case then our model based on a BCS-contact pairing Hamiltonian should be applicable. In these compounds, the paramagnetic effects seem to be rather weak: the parameter $\alpha$ varies from 0.10 for $x=0$ to 0.15 for $x=1$ (using the data from Ref. 38). This explains why the experimental $H_{c2}$ curves in these materials show a good agreement with the Helfand-Werthamer theory. Still, the absence of inversion symmetry should manifest itself in a long-wavelength helical modulation of the order parameter along the applied field. Using the maximum values of the SO band splitting from Ref. 36, we have $E_{SO} \simeq 30$ meV in $Li_2Pd_3B$ and $E_{SO} \simeq 200$ meV in $Li_2Pt_3B$. Then one can obtain the following order-of-magnitude estimates for the wave vector of the helical modulation: $q_z\xi_0 \sim 10^{-3} H/H_{c2}(0)$ in $Li_2Pd_3B$, and $q_z\xi_0 \sim 10^{-2} H/H_{c2}(0)$ in $Li_2Pt_3B$.

## ACKNOWLEDGMENTS

The author is pleased to thank V. P. Mineev for stimulating discussions. The financial support from the Natural Sciences and Engineering Research Council of Canada is gratefully acknowledged.

## APPENDIX: SPECTRUM OF $\hat{\mathcal{Y}}_{00}(\omega_n)$

The problem of finding the upper critical field is reduced to the calculation of the average normal-state Green's function in a uniform magnetic field. The difference from the centrosymmetric case is due to the presence of the SO coupling term in the Hamiltonian (8). Following Ref. 39, we represent the Green's function before disorder averaging in a factorized form:

$$G_{\alpha\beta}(\boldsymbol{r}_1,\boldsymbol{r}_2;\omega_n) = \bar{G}_{\alpha\beta}(\boldsymbol{r}_1,\boldsymbol{r}_2;\omega_n) e^{i\varphi(\boldsymbol{r}_1,\boldsymbol{r}_2)}, \tag{A1}$$

where $\varphi(\boldsymbol{r}_1,\boldsymbol{r}_2) = (e/c)\int_{r_1}^{r_2} \boldsymbol{A}(\boldsymbol{r})d\boldsymbol{r}$, and the integration is performed along a straight line connecting $\boldsymbol{r}_1$ and $\boldsymbol{r}_2$. From Eq. (12) we obtain an equation for the gauge-invariant factor,

$$(i\omega_n - \hat{\bar{h}}_1)\hat{\bar{G}}(\boldsymbol{r}_1,\boldsymbol{r}_2;\omega_n) = \delta(\boldsymbol{r}_1 - \boldsymbol{r}_2), \tag{A2}$$

where

$$\hat{\bar{h}}_1 = \frac{\bar{\boldsymbol{K}}_1^2}{2m^*} + \gamma_0 \bar{\boldsymbol{K}}_1 \hat{\boldsymbol{\sigma}} + \frac{g}{2}\mu_B \boldsymbol{H}\hat{\boldsymbol{\sigma}} + U(\boldsymbol{r}_1) - \epsilon_F, \tag{A3}$$

and $\bar{\boldsymbol{K}}_1 = -i\boldsymbol{\nabla}_1 + (e/2c)\boldsymbol{H}\times(\boldsymbol{r}_1 - \boldsymbol{r}_2)$.

As discussed in Sec. II A, in the limit of weak SO coupling it is sufficient to consider only the singlet-singlet terms in the Cooper impurity ladder. After disorder averaging, the kernel (34) takes the following form:

$$\mathcal{Y}_{00}(\boldsymbol{r}_1,\boldsymbol{r}_2;\omega_n) = \bar{\mathcal{Y}}_{00}(\boldsymbol{r}_1 - \boldsymbol{r}_2,\omega_n) e^{2i\varphi(\boldsymbol{r}_1,\boldsymbol{r}_2)}, \tag{A4}$$

where the translationally invariant part is defined by its Fourier transform as follows:

$$\bar{\mathcal{Y}}_{00}(\boldsymbol{q},\omega_n) = \frac{1}{2\pi N_F} \times \int \frac{d^3\boldsymbol{k}}{(2\pi)^3} \mathrm{tr}[\hat{\bar{G}}(\boldsymbol{k}+\boldsymbol{q},\omega_n)\hat{\sigma}_2 \hat{\bar{G}}^T(-\boldsymbol{k},-\omega_n)\hat{\sigma}_2]. \tag{A5}$$

The Green's functions here are disorder-averaged solutions of Eq. (A2). The next step is to use the identity

$e^{2i\varphi(\mathbf{r}_1,\mathbf{r}_2)}\eta(\mathbf{r}_2)=e^{-i(\mathbf{r}_1-\mathbf{r}_2)\mathbf{D}_1}\eta(\mathbf{r}_1)$, where $\mathbf{D}=-i\nabla+(2e/c)\mathbf{A}$, from which it follows that the operator $\hat{\mathcal{Y}}_{00}(\omega_n)$ can be obtained from $\overline{\mathcal{Y}}_{00}(\mathbf{q},\omega_n)$ by replacing $\mathbf{q}\to\mathbf{D}$. The gauge-invariant part of the Green's function contains the effects of the SO coupling, the Zeeman interaction, the orbital Landau quantization, and disorder. We treat the magnetic-field effects on $\hat{\bar{G}}$ perturbatively, which is legitimate if the Zeeman energy is small compared with the SO band splitting, i.e., $(g/2)\mu_B H \ll E_{\mathrm{SO}}$, and also if the temperature is not very low so that the Landau-level quantization can be neglected.

In the clean case, keeping only the terms linear in $H$ in Eq. (A2), we have

$$(i\omega_n-\hat{h}_0+\boldsymbol{H}\hat{\boldsymbol{m}})\hat{\bar{G}}(\mathbf{r},\omega_n)=\delta(\mathbf{r}), \tag{A6}$$

where $\hat{h}_0=\epsilon_0(-i\nabla)+\boldsymbol{\gamma}(-i\nabla)\hat{\boldsymbol{\sigma}}$ is the zero-field Hamiltonian, and $\hat{\boldsymbol{m}}=-\mu_B[(g/2)\hat{\boldsymbol{\sigma}}+(\boldsymbol{R}\times\hat{\boldsymbol{\pi}})]$, with $\hat{\boldsymbol{\pi}}=(m/m^*)(-i\nabla)+m\gamma_0\hat{\boldsymbol{\sigma}}$, has the meaning of the magnetic-moment operator for band electrons. The eigenvalues of $\hat{h}_0$ are given by $\xi_\lambda(\boldsymbol{k})$ [see Eq. (4)]. It is straightforward to show that the linear in $H$ effects on $\hat{\bar{G}}$ are due to the Zeeman interaction (the first term in $\hat{\boldsymbol{m}}$). Then, $\hat{\bar{G}}(\boldsymbol{k},\omega_n)$ can be represented in the form (13), with the band Green's functions now given by

$$G_\lambda(\boldsymbol{k},\omega_n)=\frac{1}{i\omega_n-\xi_\lambda(\boldsymbol{k})-\lambda(g/2)\mu_B\hat{\boldsymbol{k}}\boldsymbol{H}}. \tag{A7}$$

Thus, the electron bands are deformed by the magnetic field: $\xi_\lambda(\boldsymbol{k})\to\xi_\lambda(\boldsymbol{k})+\lambda(g/2)\mu_B\hat{\boldsymbol{k}}\boldsymbol{H}$.

In the presence of impurities, again keeping the magnetic field only in the Zeeman term in Eq. (A3), we obtain for the average Green's function,

$$\hat{\bar{G}}(\boldsymbol{k},\omega_n)=[i\omega_n-\epsilon_0(\boldsymbol{k})-\tilde{\boldsymbol{\gamma}}(\boldsymbol{k})\hat{\boldsymbol{\sigma}}-\hat{\Sigma}_{\mathrm{imp}}(\omega_n)]^{-1}, \tag{A8}$$

where $\tilde{\boldsymbol{\gamma}}(\boldsymbol{k})=\gamma_0\boldsymbol{k}+(g/2)\mu_B\boldsymbol{H}$, and

$$\hat{\Sigma}_{\mathrm{imp}}(\omega_n)=n_{\mathrm{imp}}U_0^2\int\frac{d^3u}{(2\pi)^3}\hat{\bar{G}}(\boldsymbol{k},\omega_n) \tag{A9}$$

is the impurity self-energy in the self-consistent Born approximation. We seek the self-energy matrix in a spin-diagonal form: $\hat{\Sigma}_{\mathrm{imp}}(\omega_n)=-i\beta(\omega_n)\hat{\sigma}_0$. Then, $\hat{\bar{G}}(\boldsymbol{k},\omega_n)=\Sigma_\lambda\hat{\Pi}_\lambda(\boldsymbol{k})G_\lambda(\boldsymbol{k},\tilde{\omega}_n)$, where $\tilde{\omega}_n=\omega_n+\beta(\omega_n)$, and the band projection operators and the band Green's function are given by expressions (14) and (A7), respectively. Substituting this into Eq. (A9) and neglecting the energy dependence of the band densities of states on the scale of the Zeeman energy, we find $\tilde{\omega}_n=\omega_n+\Gamma\ \mathrm{sign}\ \omega_n$. Therefore,

$$\hat{\bar{G}}(\boldsymbol{k},\omega_n)=\sum_\lambda\hat{\Pi}_\lambda(\boldsymbol{k})\times\frac{1}{i\omega_n-\xi_\lambda(\boldsymbol{k})-\lambda(g/2)\mu_B\hat{\boldsymbol{k}}\boldsymbol{H}+i\Gamma\ \mathrm{sign}\ \omega_n}. \tag{A10}$$

Inserting the last expression in Eq. (A5), we obtain

$$\overline{\mathcal{Y}}_{00}(\boldsymbol{q},\omega_n)=\frac{1}{2}\sum_\lambda\rho_\lambda\left\langle\frac{1}{|\omega_n|+\Gamma+i\Omega_\lambda\ \mathrm{sign}\ \omega_n}\right\rangle_{\hat{\boldsymbol{k}}}, \tag{A11}$$

where $\rho_\lambda=N_\lambda/N_F$, and $\Omega_\lambda(\boldsymbol{k},\boldsymbol{q})=v_F\hat{\boldsymbol{k}}(\boldsymbol{q}+\lambda g\mu_B\boldsymbol{H}/v_F)/2$. Next we use in Eq. (A11) the identity $a^{-1}=\int_0^\infty du\ e^{-au}$ and make the substitution $\boldsymbol{q}\to\boldsymbol{D}$ to represent $\hat{\mathcal{Y}}_{00}(\omega_n)$ as a differential operator of infinite order,

$$\hat{\mathcal{Y}}_{00}(\omega_n)=\frac{1}{2}\int_0^\infty du\ e^{-u(|\omega_n|+\Gamma)}\sum_\lambda\rho_\lambda\hat{\mathcal{O}}_\lambda. \tag{A12}$$

Here

$$\hat{\mathcal{O}}_\lambda=\left\langle\exp\left[-\frac{iuv_F}{2}\hat{\boldsymbol{k}}\left(\boldsymbol{D}+\lambda\frac{g\mu_B\boldsymbol{H}}{v_F}\right)\right]\right\rangle_{\hat{\boldsymbol{k}}} \tag{A13}$$

do not depend on $\omega_n$ because the zero-field Fermi surfaces are invariant under $\boldsymbol{k}\to-\boldsymbol{k}$.

To find the eigenfunctions and eigenvalues of $\hat{\mathcal{O}}_\lambda$, we follow the procedure outlined in Ref. 16. We choose the $z$ axis along the external field so that $\boldsymbol{H}=H\hat{z}$, and introduce the operators

$$a_\pm=\ell_H\frac{D_x\pm iD_y}{2},\quad a_3=\ell_H D_z, \tag{A14}$$

where $\ell_H=\sqrt{c/eH}$ is the magnetic length. It is easy to check that $a_+=a_-^\dagger$ and $[a_-,a_+]=1$; therefore $a_\pm$ have the meaning of the raising and lowering operators while $a_3=a_3^\dagger$ commutes with both of them: $[a_3,a_\pm]=0$. We use the basis of states $|N,p\rangle$ (Landau levels), such that

$$a_+|N,p\rangle=\sqrt{N+1}|N+1,p\rangle,$$

$$a_-|N,p\rangle=\sqrt{N}|N-1,p\rangle,$$

$$a_3|N,p\rangle=p|N,p\rangle,$$

where $N=0,1,\ldots$, and $p$ is a real number. Then,

$$\begin{aligned}\hat{\mathcal{O}}_\lambda|N,p\rangle&=\frac{1}{2}\int_0^\pi d\theta\ \sin\theta e^{-iv(p+\lambda p_0)\cos\theta}\\&\times\int_0^{2\pi}\frac{d\phi}{2\pi}e^{-iv\ \sin\theta(e^{-i\phi}a_++e^{i\phi}a_-)}|N,p\rangle\\&=\frac{1}{2}\int_{-1}^1 ds\ e^{-iv(p+\lambda p_0)s}e^{-(v^2/2)(1-s^2)}\\&\times L_N[v^2(1-s^2)]|N,p\rangle,\end{aligned} \tag{A15}$$

where $v=(v_F/2\ell_H)u$, $p_0=g\mu_B H\ell_H/v_F$, and $L_N(x)$ is the Laguerre polynomial of degree $N$. We see that the Landau levels $|N,p\rangle$ are eigenfunctions of $\hat{\mathcal{O}}_\lambda$ and, therefore, of $\hat{\mathcal{Y}}_{00}(\omega_n)$. Introducing $\delta=(\rho_+-\rho_-)/2$ and summing over $\lambda$ in Eq. (A12), we arrive at expression (36).

[1] E. Bauer, G. Hilscher, H. Michor, Ch. Paul, E. W. Scheidt, A. Gribanov, Yu. Seropegin, H. Noël, M. Sigrist, and P. Rogl, Phys. Rev. Lett. **92**, 027003 (2004).
[2] K. Togano, P. Badica, Y. Nakamori, S. Orimo, H. Takeya, and K. Hirata, Phys. Rev. Lett. **93**, 247004 (2004); P. Badica, T. Kondo, and K. Togano, J. Phys. Soc. Jpn. **74**, 1014 (2005).
[3] V. M. Edelstein, Zh. Eksp. Teor. Fiz. **95**, 2151 (1989) [Sov. Phys. JETP **68**, 1244 (1989)].
[4] L. P. Gor'kov and E. I. Rashba, Phys. Rev. Lett. **87**, 037004 (2001).
[5] S. K. Yip, Phys. Rev. B **65**, 144508 (2002).
[6] P. A. Frigeri, D. F. Agterberg, A. Koga, and M. Sigrist, Phys. Rev. Lett. **92**, 097001 (2004); **93**, 099903(E) (2004).
[7] P. A. Frigeri, D. F. Agterberg, and M. Sigrist, New J. Phys. **6**, 115 (2004).
[8] K. V. Samokhin, Phys. Rev. Lett. **94**, 027004 (2005).
[9] K. V. Samokhin, Phys. Rev. B **76**, 094516 (2007).
[10] L. S. Levitov, Yu. V. Nazarov, and G. M. Eliashberg, Pis'ma Zh. Eksp. Teor. Fiz. **41**, 365 (1985) [JETP Lett. **41**, 445 (1985)].
[11] V. M. Edelstein, Phys. Rev. Lett. **75**, 2004 (1995).
[12] S. Fujimoto, Phys. Rev. B **72**, 024515 (2005).
[13] D. F. Agterberg, Physica C **387**, 13 (2003).
[14] K. V. Samokhin, Phys. Rev. B **70**, 104521 (2004).
[15] R. P. Kaur, D. F. Agterberg, and M. Sigrist, Phys. Rev. Lett. **94**, 137002 (2005).
[16] E. Helfand and N. R. Werthamer, Phys. Rev. **147**, 288 (1966).
[17] N. R. Werthamer, E. Helfand, and P. C. Hohenberg, Phys. Rev. **147**, 295 (1966).
[18] C. T. Rieck, K. Scharnberg, and N. Schopohl, J. Low Temp. Phys. **84**, 381 (1991).
[19] V. Barzykin and L. P. Gor'kov, Phys. Rev. Lett. **89**, 227002 (2002).
[20] O. Dimitrova and M. V. Feigel'man, Phys. Rev. B **76**, 014522 (2007).
[21] V. P. Mineev and K. V. Samokhin, Phys. Rev. B **75**, 184529 (2007).
[22] E. I. Rashba, Fiz. Tverd. Tela (Leningrad) **2**, 1224 (1960) [Sov. Phys. Solid State **2**, 1109 (1960)].
[23] K. V. Samokhin and V. P. Mineev, Phys. Rev. B **77**, 104520 (2008).
[24] E. M. Lifshitz and L. P. Pitaevskii, *Statistical Physics* (Butterworth-Heinemann, Oxford, 1995), Pt. 2.
[25] A. A. Abrikosov, L. P. Gorkov, and I. E. Dzyaloshinski, *Methods of Quantum Field Theory in Statistical Physics* (Dover, New York, 1975).
[26] K. V. Samokhin, Phys. Rev. B **78**, 144511 (2008).
[27] K. Maki, Physics **1**, 127 (1964).
[28] L. P. Gor'kov, Zh. Eksp. Teor. Fiz. **37**, 1407 (1959) [Sov. Phys. JETP **10**, 998 (1960)].
[29] A. I. Larkin and Yu. N. Ovchinnikov, Zh. Eksp. Teor. Fiz. **47**, 1136 (1964) [Sov. Phys. JETP **20**, 762 (1965)]; P. Fulde and R. A. Ferrell, Phys. Rev. **135**, A550 (1964).
[30] D. F. Agterberg and R. P. Kaur, Phys. Rev. B **75**, 064511 (2007).
[31] One should keep in mind that Eq. (51) and subsequent results are valid only if the Zeeman energy is small compared with the SO band splitting, i.e., at $\tilde{h} \ll E_{\mathrm{SO}}/T_{c0}$.
[32] M. Tinkham, *Introduction to Superconductivity* (McGraw-Hill, New York, 1996), Chap. 10.2.
[33] A. M. Clogston, Phys. Rev. Lett. **9**, 266 (1962); B. S. Chandrasekhar, Appl. Phys. Lett. **1**, 7 (1962).
[34] L. W. Gruenberg and L. Gunther, Phys. Rev. Lett. **16**, 996 (1966).
[35] L. G. Aslamazov, Zh. Eksp. Teor. Fiz. **55**, 1477 (1968) [Sov. Phys. JETP **28**, 773 (1969)].
[36] K.-W. Lee and W. E. Pickett, Phys. Rev. B **72**, 174505 (2005).
[37] H. Q. Yuan, D. F. Agterberg, N. Hayashi, P. Badica, D. Vandervelde, K. Togano, M. Sigrist, and M. B. Salamon, Phys. Rev. Lett. **97**, 017006 (2006); M. Nishiyama, Y. Inada, and G.-Q. Zheng, *ibid.* **98**, 047002 (2007).
[38] P. S. Häfliger, R. Khasanov, R. Lortz, A. Petrović, K. Togano, C. Baines, B. Graneli, and H. Keller, arXiv:0709.3777 (unpublished).
[39] L. P. Gor'kov, Zh. Eksp. Teor. Fiz. **36**, 1918 (1959) [Sov. Phys. JETP **9**, 1364 (1959)].